Fibers and Polymers 2017, Vol.18, No.2, 303-312
DOI 10.1007/s12221-017-6067-5

ISSN 1229-9197 (print version)
ISSN 1875-0052 (electronic version)

Comparative Investigation of Molded Thickness and Surface Density on the Structures and Mechanical Properties of Lightweight Reinforced Thermoplastic Composites

Xun Fang, Chunyin Shen*, and Gance Dai

State Key Laboratory of Chemical Engineering, East China University of Science and Technology, Shanghai 200237, China
(Received January 22, 2016; Revised November 8, 2016; Accepted November 16, 2016)

Abstract: Lightweight reinforced thermoplastic (LWRT) is a newly developed porous material. The low density, high rigidity, design flexibility and sound absorption of LWRT facilitate its application in the automotive industry. Fibers are bonded with a matrix and air is imported by deconsolidation, which is not only economical but also environmentally friendly. In this work, film stacking and non-woven methods were employed as the impregnation techniques to manufacture LWRT. The molded thickness and surface density of LWRT were varied to study their influences on the structures and mechanical properties. Different lengths of fibers in LWRT were selected and 7 % PP-g-MAH was added to the matrix and compared with unmodified matrix. The mechanical properties decreased with the increase in molded thickness and the decrease in surface density. With higher fiber length, the strength and stiffness increased, while the toughness exhibited a maximum value at 80 mm fiber length. The strength and stiffness of LWRT were also enhanced when 7 % PP-g-MAH was added.

Keywords: Lightweight, Porous, Deconsolidation, Fiber length, Compatibilizer

Introduction

Glass mat reinforced thermoplastic (GMT) has been widely used in the automobile industry, including in bumper beams, load floors, and pallets, owing to its outstanding performance. Lightweight reinforced thermoplastic (LWRT) composites are considered the new generation of GMT. The advantages of LWRT are very attractive, including potential weight reduction. Typically, GMT weighs 4 to 5 kg/m^2, while LWRT weighs 0.5 to 2 kg/m^2. However, the low density of LWRT produces higher stiffness per unit weight than a traditional GMT sheet. The short molding cycle time, recyclability, and environmentally friendly manufacturing process of LWRT are also appealing. LWRT also provides perfect sound and energy insulation properties, extends design freedom and has the ability to form into complex shapes in one-step easy molding with fabric and other trims. Together, these advantages have made applications of LWRT in automotive interior parts, such as headliners, instrument panels and load floors, promising [1].

Generally, in porous materials, bubbles are generated by adding blowing agents in traditional foam plastics [2-5]. These blowing agents are either physical or chemical agents. They are expensive and the residue may be harmful. Bubbles in syntactic foams are produced by adding hollow microspheres [6,7]. The small particle size may cause industrial disease, and the toughness is usually reduced with more hollow glass beads. The method of introducing bubbles in LWRT is novel and is inspired by the reprocessing of thermoplastic composites. Thermoplastic composites may suffer an increase in thickness and porosity during post-thermal processing when the temperature is above the melt temperature. This phenomenon is called deconsolidation [8-13] or lofting. It can be interpreted as the inverse process of consolidation. Air is inhaled when resin is melted and compressed fiber mats rebound. In this way, a porous structure is obtained. This process is not only economical but also environmentally friendly.

A wet process [14] and dry process [15] are found to be suitable means of manufacturing LWRT. The former is similar to papermaking, but the dispersing fluid is aqueous foam. The dispersed mixture of glass fiber and polypropylene is then pumped onto a forming belt. After vacuum treatment, a uniform fibrous web is produced. The fibrous web is heated and semi-consolidated by a set of nip rollers after drying. The dry process borrows techniques from textile manufacturing. Polypropylene fiber and glass fiber are commingled. The formed mats are needled, then heated and consolidated. After a low-pressure thermoforming process, the solid blanks transform to the finished parts.

The microstructure of LWRT is much more complex than that of traditional GMT, which has been studied in depth. Because LWRT is formed with fiber, matrix and air, the macroscopic properties are greatly affected by the synergy and interference among the components. If the fiber-matrix interface is continuous, the fiber will greatly reinforce the matrix. However, if the fiber-matrix interface is interrupted by air, the strength will decrease. In this paper, the LWRT structure is discussed and some factors are provided to study the synergy and interference.

Experimental

Raw Materials

Polypropylene Y2600 purchased from Sinopec Shanghai Petrochemical Company Limited was used as the matrix.

*Corresponding author: ichuny@ecust.edu.cn

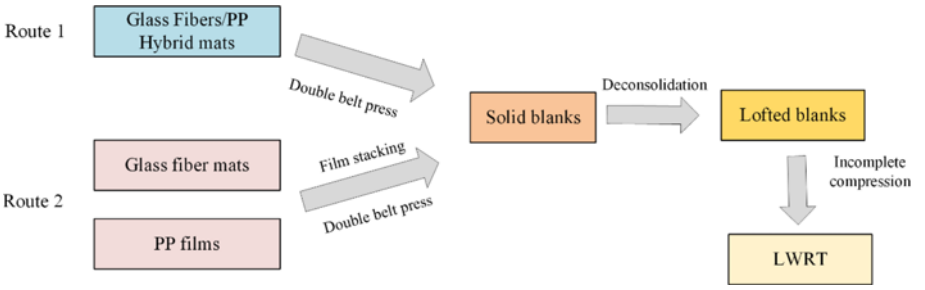

Figure 1. The manufacturing procedure of LWRT.

Maleic anhydride grafted polypropylene (MAH-g-PP) was obtained from Shanghai Yuanyuan Polymer Material Science and Technology Co., Ltd. Antioxidants Irganox 1010 and Irgfos 168 were purchased from Ciba Specialty Chemicals Corporation (Switzerland), while glass rovings ER13-2000-950 were supplied by Jushi Group Company Limited.

Manufacturing

LWRT was made from GMT solid blanks. The latter underwent a process of deconsolidation and transformed to LWRT by incomplete compression. The procedure is illustrated in Figure 1. Therefore, the first step was to manufacture GMT solid blanks.

Preparation of Solid Blanks

In this paper, two methods were applied to prepare solid blanks. One is the film stacking method [16], while the other is the non-woven technique [17].

During the film stacking process, a twin-screw extruder was selected to blend the PP granules and the antioxidants. The temperature was set to 165-220 °C, and the screw speed was 120 r/min. After using a three-roll calender, matrix films were obtained. Then, three-layer films and two-layer needled long glass fiber mats were laid alternately and sent to the double belt press. The three zones in the double belt press are the pre-heating zone, the hot pressing zone and the cold pressing zone. During pre-heating, the temperature was set to 220 °C, and the matrix films were heated to form a melt. The hot press provided a pressure of 1.0 MPa for melt impregnation, and the cold press was set to the ambient temperature so that the matrix could solidify.

During the non-woven process, the PP matrix was blended with antioxidants in a mixer at 220 °C and spun into yarns by a spinning machine. Then, polypropylene yarns and glass rovings at a mass ratio of 1:1 were cut to a certain length and fed into a carding machine after being preliminary blended. Different fiber lengths used to compare with each other respectively were 40 mm, 60 mm, 80 mm, 100 mm and 120 mm. The hybrid non-woven webs were obtained from the carding machine. The two types of fibers were mixed uniformly and dispersed into monofilaments after the carding process. After layup and needle-punching, hybrid mats were manufactured. They were sent to the double belt press and consolidated.

By comparison, the non-woven technique has advantages in impregnation. Because the glass fiber content in LWRT is high to ensure deconsolidation, the flow resistance of the resin is very large. For the film stacking process, the resin must flow longer to accomplish the impregnation process. However, this seems to be easier for the non-woven technique since the resin can impregnate fibers easily. Therefore, the non-woven technique is preferred.

Preparation of LWRT

The solid blanks were heated in an oven for 8 min at a temperature of 220 °C, and they underwent a deconsolidation process. The thickness of the blanks increased to 12 mm. Then, the blanks were transferred to a plate vulcanizing press and compressed to a certain thickness under a pressure of 10 MPa. The mass fraction of glass fibers in LWRT was 50 % and the thickness of LWRT varied from 2 mm to 5.5 mm. The surface density of 2000 g/m^2 was used to compare with 1400 g/m^2.

Mechanical Testing

Five samples were prepared by standard cutters for each test. The tensile testing was conducted according to ISO 527-2012. The testing apparatus was a CMT 4204 universal testing machine manufactured by Shenzhen SANS Experimental Equipment Corp., Ltd. The analysis was performed at a constant crosshead speed of 5 mm/min. An extensometer with gauge length of 50 mm was used for the modulus measurements.

The flexural testing was performed on a CMT 4204 universal testing machine under three-point loading according to ISO 178-2010. Flexural samples with a width of 10 mm and length of 100 mm were prepared. The span length between two supporting noses was 80 mm and a crosshead speed of 5 mm/min was used.

The notched Izod impact test was performed on a cantilever beam impact machine according to standard ISO 180-2000. Impact specimens with a remaining width of 8 mm at the notch base were prepared.

Morphology Characterization

LWRT is a multiphase system that consists of the matrix,

fiber and air. The morphology of LWRT is quite complex. A scanning electron microscope (Nova NanoSEM 450) by FEI Company with an accelerating voltage of 3 kV was used to observe the morphology of LWRT. Before examination, the non-conductive samples were sputter coated with a thin layer of platinum. The pore feature was characterized with a digital microscope (KH8700) by Hirox China Co., Ltd. The depths of field caused by the uneven topography can be measured. Pictures with different depths of field were stacked to build the 3D morphology.

Results and Discussion

Pores and Their Formation

Figure 2(a) shows the surface morphology of LWRT. There are a number of pores on the surface of LWRT with variable sizes and a shape that is close to an ellipse. Through these pores, crisscrossed fibers can be observed inside the material. After deconsolidation, LWRT suffered a compression process in order to achieve a certain thickness; then, the resin melt is spread on the fibers, but the flow front is unable to converge before solidification, causing the pore shape to be formed. The exposed fibers also act as the boundaries of pores.

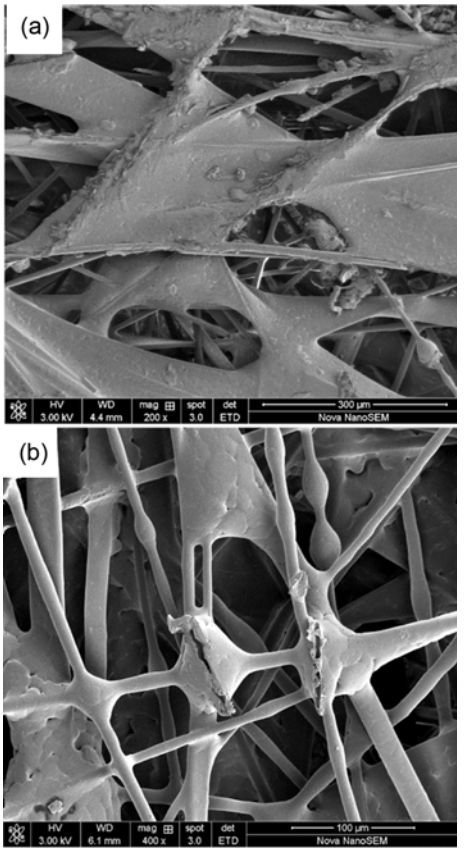

Figure 2. SEM photos of the surface and interior morphology; (a) surface morphology and (b) interior morphology.

Figure 2(b) shows the interior morphology of LWRT. The interior, which is a multiphase system, consists of the matrix, fiber and air. The pores are interconnected. Some resins flow along the axis of the fibers and converge at the fiber intersections. Some resins flow perpendicularly to the axis of the fibers and spread between two fibers. The fibers are bonded by the resin and build the framework of LWRT in the two situations. Resin nodes at the fiber intersections are especially important in the whole structure. Stress can be transferred effectively, and strength and stiffness are both provided by this structure.

Because of the narrow visual field of SEM, a digital microscope (Hirox KH8700) was used to observe the pore features of LWRT. It has the ability to measure the depth of field accurately and reconstruct the 3D morphology by compositing the pictures with different depths of field. In this way, the pore structure can be visually displayed. Figure 3(a) shows the cross section of LWRT samples. Large numbers of long and narrow pores are apparent in the cross section. This is due to the horizontal distribution of most fibers instead of a vertical distribution, which is caused by the needling process only. As a result, fibers unwetted by the resin will form the narrow pores. This also implies that when the porosity is too large, the possibility of delamination will increase. Figure 3(b) is the longitudinal section of the LWRT samples. The uneven sizes of pores are distributed in the section, and the shapes of the pores are also irregular and are closer to an ellipse or polygon. Figures 3(c) and (d) show the 3D composite images of the longitudinal section and the contour map. The pores can be easily observed in the two images. Size and depth fluctuation are observed in the longitudinal section. The size of the pores ranges from 50 to 500 μm and the depth of pores is up to 600 μm. However, this technology has a limitation in that the information of the under layer is often covered by the upper layer. The integrated pore structures may be characterized by more advanced technology, such as μCT [18].

Pores are formed by a deconsolidation process that is typical for LWRT. Before lofting, fiber mats are under compression and the solidified resin restrains the springback of fibers. During deconsolidation, the resin becomes a melt and relieves the constraint; then, the fibers rebound where air is inhaled from the outside and pores in the LWRT are formed. There is an analogy between fiber mats and springs. Many factors can affect the deconsolidation process, such as fiber content, fiber length and needling. If the fibers are too short, they hardly form the framework. If the fiber mats are not needled, vertical fibers will be lacking and elastic potential energy cannot be stored. However, if the fibers are too long or if they are needled too much, the connections among the fibers will be excessive and the elasticity of the mats will decrease. The conditions above are all detrimental to the deconsolidation process. Moreover, the heating temperature and time also affect deconsolidation and the

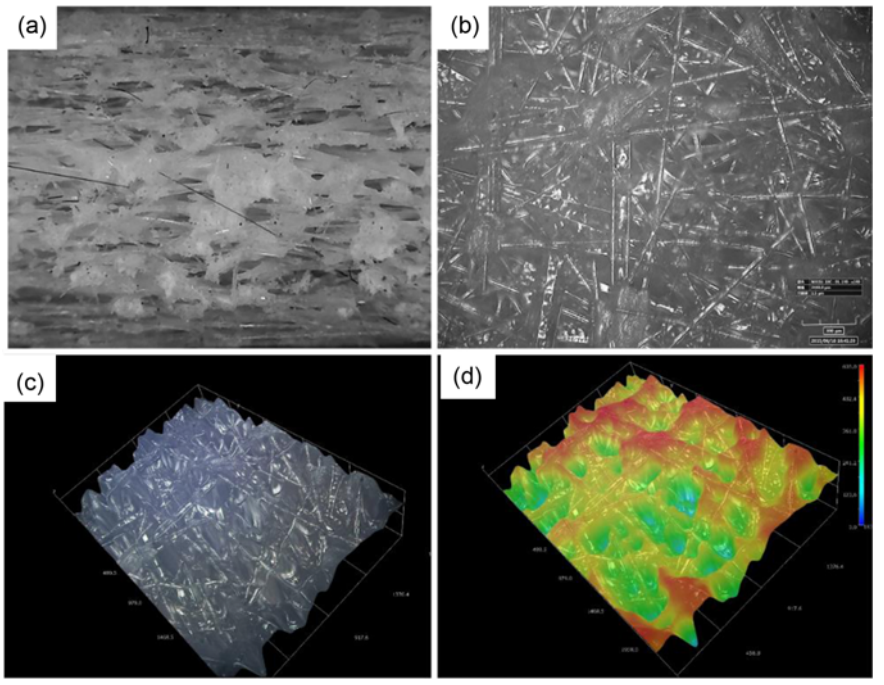

Figure 3. Morphology of the cross section and longitudinal section; (a) cross section, (b) longitudinal section, (c) 3D composite image, and (d) contour map.

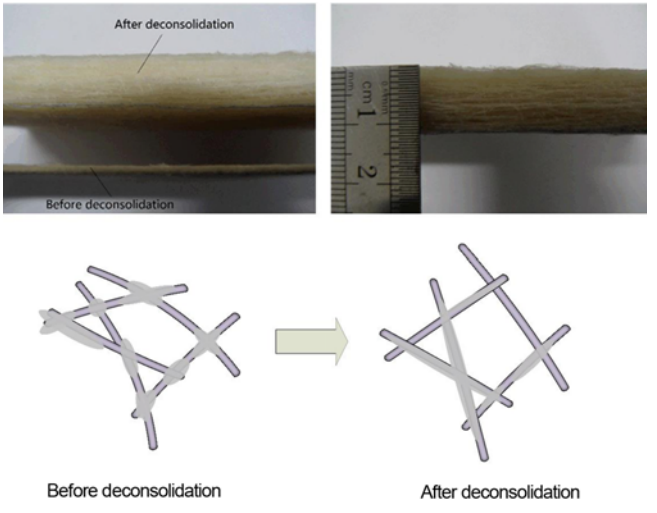

Figure 4. Deconsolidation (lofting) of LWRT.

formation of pores.

The polypropylene/glass fiber hybrid mats with surface density of 1400 g/m^2 and fiber content of 50 % by weight were prepared by the non-woven technique. The lofted thickness of this type of mat will reach 12 mm, while the consolidated sheet is only 1 mm thick. As a result, the molded thickness can vary from 1 mm to 12 mm. The phenomenon of deconsolidation is shown in Figure 4.

Designability of LWRT - Thickness and Surface Density

LWRT has very high designability due to its unique formation method. Both the thickness and surface density are adjustable. The lofted thickness can be molded back to a certain thickness according to the requirement. With the same thickness, different surface densities also provide different properties. The two major design factors are both connected to the porosity of LWRT. With the increase of thickness and the decrease of surface density, the porosity of LWRT increases. The porosity ϕ of LWRT can be estimated through equation (1):

$$\phi = 1-\rho\left(\frac{m_m}{\rho_m}+\frac{m_f}{\rho_f}\right) = 1-\frac{s}{h}\left(\frac{m_m}{\rho_m}+\frac{m_f}{\rho_f}\right) \quad (1)$$

where ρ is the density of LWRT which equals to the surface density s divided by thickness h, ρ_f and ρ_m are the densities of the fibers and matrix, respectively, and m_f and m_m are the mass fractions of the fibers and matrix, respectively. When the surface density of LWRT is 1400 g/m^2 and the mass fraction of fibers is 50 %, the porosity changes with the thickness as shown in Figure 5. The porosity increases with the thickness, but changes little when the thickness is large.

Figures 6(a) and (b) illustrate the influences of thickness on the tensile and flexural properties of LWRT. Both the tensile properties and flexural properties decrease with the thickness, but the variation tendency becomes slower, which is very similar to the increasing tendency of porosity. Figure 7 shows the tensile failure modes of LWRT with different thicknesses. When the thickness is small, tensile fracture occurs due to fiber breakage and matrix cracking. With the increase of the thickness, delamination failure tends to occur

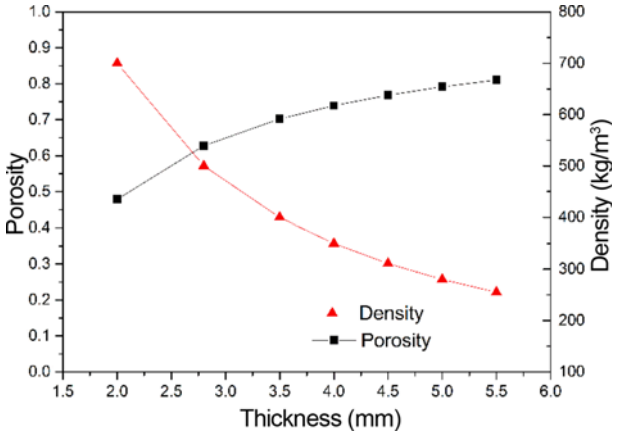

Figure 5. Relationship between thickness and porosity (1400 g/m^2, 50 %).

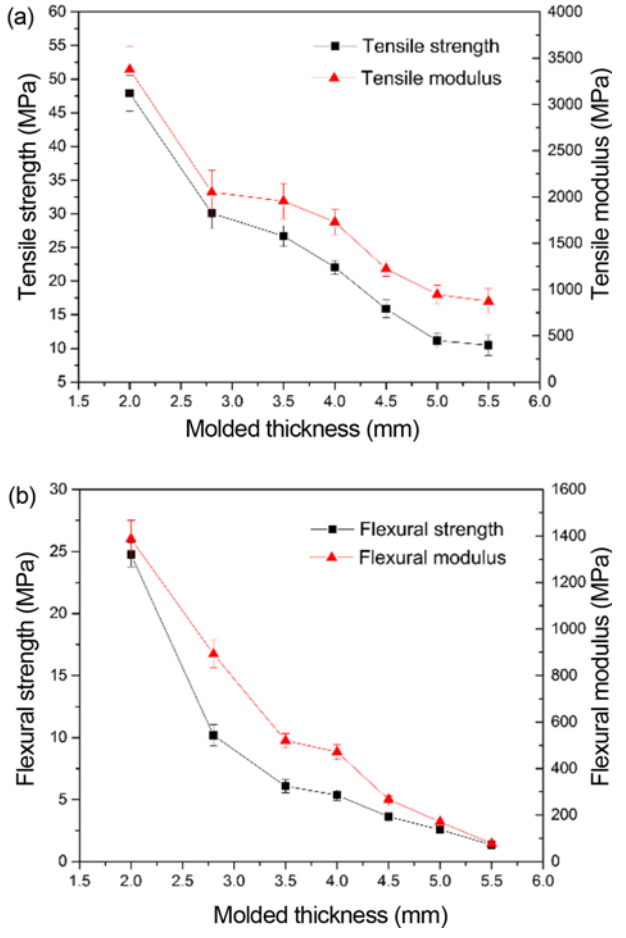

Figure 6. Influence of thickness on the tensile and flexural properties; (a) tensile properties and (b) flexural properties.

because the interlaminar bonding is weak.

Although the flexural modulus decreases with the thickness, this does not mean the flexural stiffness of LWRT is low. As illustrated in Figure 8, the maximum value of the flexural

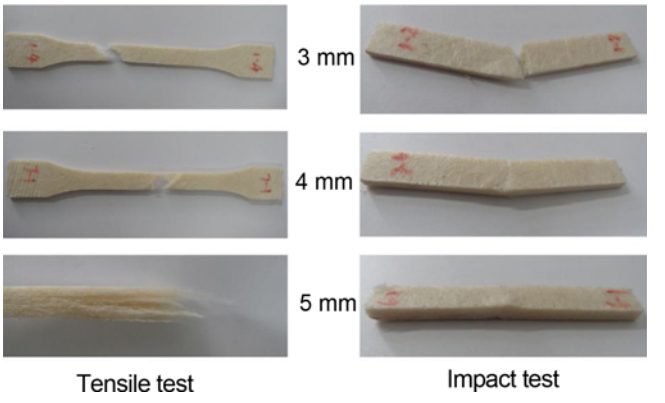

Figure 7. Failure modes of tensile and impact.

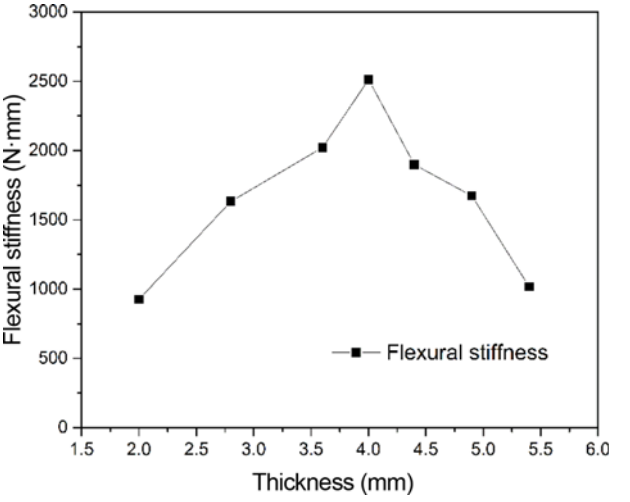

Figure 8. Influence of thickness on the flexural stiffness of LWRT.

stiffness occurs with the increase of thickness. The result shows the difference between modulus and stiffness. Equation (2) is used to calculate the flexural stiffness:

$$S = EI/b = (h^3/12)E \quad (2)$$

where E is the modulus, I is the moment of inertia to the central axis of rectangular sections which equals $bh^3/12$, b is the width and h is the thickness of the sample. The flexural stiffness is decided by the thickness aside from the modulus. When the thickness increases, the modulus is decreased. The two contrasting effects make the flexural stiffness increase in the first stage but decrease in the latter stage. The highest stiffness occurs at 4 mm thickness.

The impact strength, as shown in Figure 9, decreases as the thickness increases, but remains constant between a thickness of 3 mm and 3.5 mm. When the thickness increases, the whole energy absorbed first increases and then decreases, as shown in Figure 9. The energy dissipation has the maximum value at a thickness of 3.5 mm. However, the impact

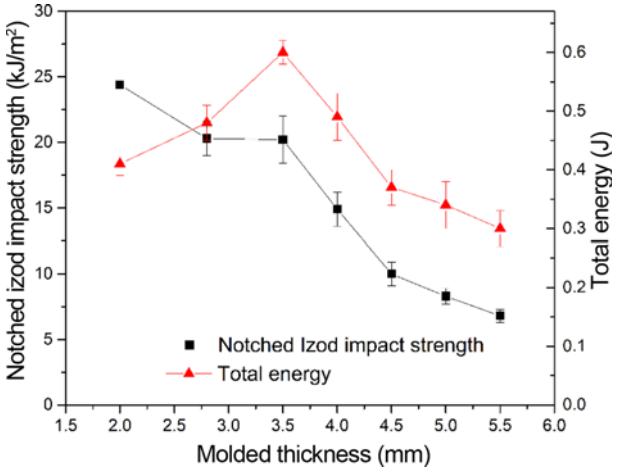

Figure 9. Influence of thickness on the impact properties of LWRT.

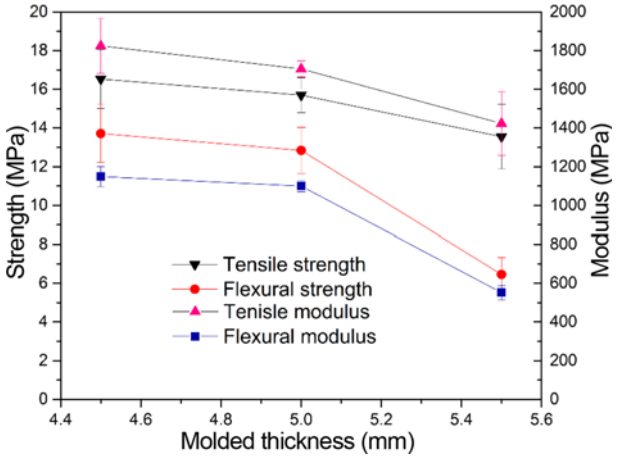

Figure 10. Mechanical properties of LWRT with a surface density of 2000 g/m^2.

strength is defined as the energy dissipation per unit area. With the increased thickness, the section area increases as well, such that the impact strength displays a decreasing trend. It can be concluded that LWRT has a good energy absorption effect within a certain range. The failure modes are illustrated in Figure 7. When the thickness is small, fracture is observed. With the increase of thickness, the energy will be dissipated by the deformation of the fiber web. The mechanism of deformation will contribute to more total energy. The sample is only partially broken. However, if the thickness becomes too large, the structure of the interlamination is weak; thus, interlaminar fracture is the major failure mode and the energy absorbed will decrease. Interlayer wrinkle is found on the section of the tested samples.

Surface density is also an important design factor. At the same thickness, a higher surface density implies lower porosity. Therefore, LWRT with a higher surface density may have higher strength and modulus. Figure 10 illustrates the strength and modulus of LWRT with a surface density of 2000 g/m^2. The tensile strength for a thickness of 5.5 mm is 13.55 MPa; however, for the same thickness, the tensile strength of LWRT with a surface density of 1400 g/m^2 is only 10.49 MPa. The porosity of LWRT with a surface density of 2000 g/m^2 is calculated to be 0.72, while the porosity with a surface density of 1400 g/m^2 is 0.86. The denser material has higher strength and modulus.

LWRT Framework - Contribution of Fiber Length

Fiber length is an important factor in discontinuous fiber reinforced composites. When the fiber length is below a critical value, fibers cannot reach the breaking stress. The strength of composites depends on the debonding length. When the fiber length is above a critical value, the fibers tend to break and the strength of composites changes slightly. Therefore, the tensile strength is usually increased with the fiber length at first but is ultimately unchanged. The toughness of fiber reinforced composites is also influenced by the fiber length. The debonding energy, the pull-out energy and the fracture strain energy stored in the debonding length all have relations with the fiber length [19]. Therefore, the fiber length in composites is a very important factor. However, the influence of fiber length in LWRT is quite different from that in voidless composites due to its unique structure. Vaikhanski [20] discussed the mechanism of fiber-reinforced polymer foams. In conventional composites, the fiber-matrix interface is continuous, resulting in efficient stress transfer between the matrix and fibers. However, in fiber-reinforced cellular composites, stress transfer between constituents is interrupted significantly by the porous structure. Thus, longer fibers are required to allow stress to fully develop along the fiber length. The biggest difference between LWRT and other composites is that fibers compose the framework of LWRT. Only fibers with a sufficient length have the ability to build a stable and strong framework. Therefore, the strength and stiffness are guaranteed.

The influences of fiber length on the tensile and flexural properties of LWRT are shown in Figures 11(a) and 11(b). The thickness of the LWRT samples is 4 mm. When the fiber length is less than 80 mm, the tensile strength increases with the fiber length. However, it becomes constant when the fiber length exceeds 80 mm. The length is much higher than the common critical length of voidless composites. This indicates that the fracture mechanism of LWRT is different from traditional composites. In LWRT, the three-dimensional web is constructed by the fibers and the resin acts as an adhesive. With longer fibers, the overlap and link between the fibers increase, and the stress can be transferred along the fibers. As a result, the strength of the fiber web is higher and the resistance to tensile stress is also higher. However, significantly longer fibers will not contribute much to the strength. The tensile and flexural moduli have a similar trend

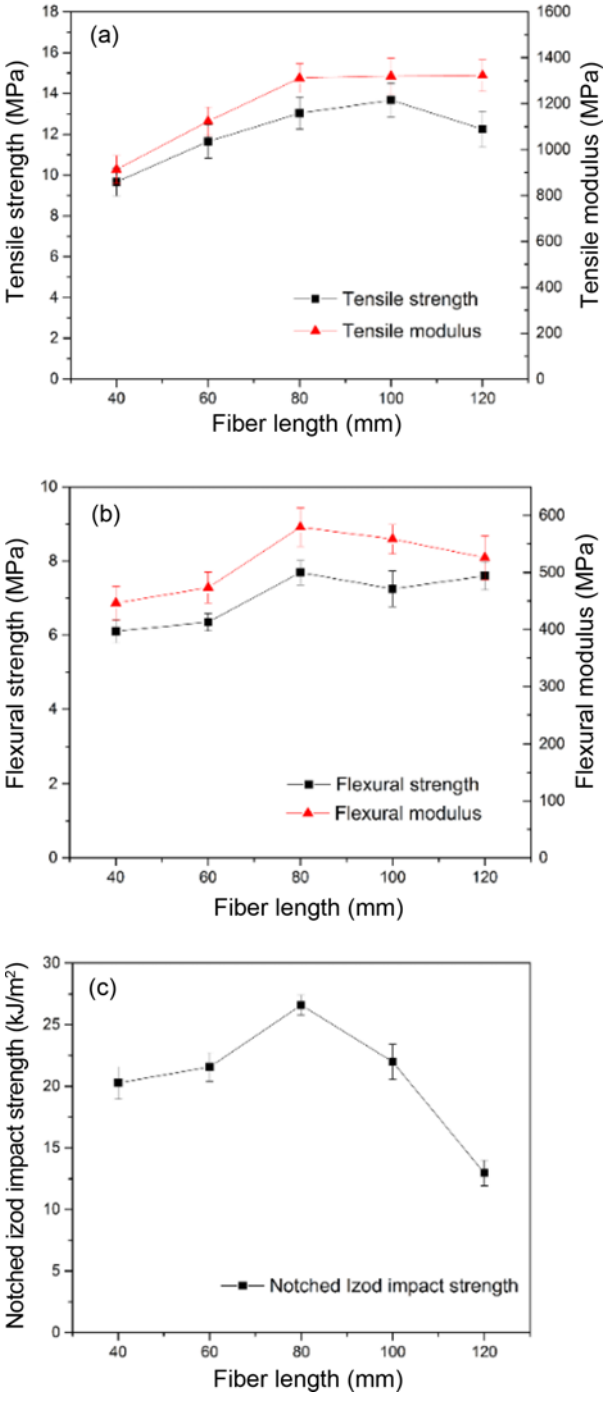

Figure 11. Influence of fiber length on the mechanical properties of LWRT; (a) tensile, (b) flexural, and (c) impact.

as the strength. This is also because the 3D web with longer fibers will exhibit higher stiffness and the resistance to deformation will increase. Figure 12(a) shows stress transfer along short fibers. Because of the discontinuity, the stress transfer will be interrupted and the strength is low. Figure 12(b) shows stress transfer along long fibers. Due to the

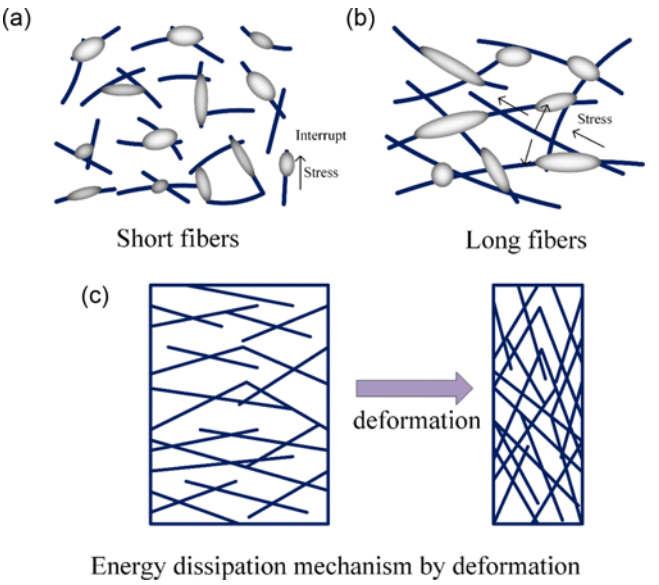

Figure 12. Effect of fiber length.

overlap and link between fibers, the stress transfer can be continued in the fiber web, and the strength is increased significantly.

The influence of fiber length on the impact property of LWRT is illustrated in Figure 11(c). With the increase of fiber length, the notched impact strength increases at first, then decreases and reaches the maximum at 80 mm fiber length. When the fiber is short, energy is dissipated by the matrix crack and fiber pull-out under the impact load. As the fiber length increases, the overlap and link of fibers make the fiber web stronger, and strain energy of the fiber web will be dissipated by deformation. This will contribute to most of the energy absorption. Figure 12(c) shows the deformation of a fiber web with a proper length which dissipates a large amount of energy. However, if the fibers are long, the constraint by surrounding fibers becomes higher and the ability to deform declines. As a result, less strain energy is dissipated by deformation of the fiber web. Fibers are broken directly and the impact strength decreases. It can be stated that longer fibers are required to improve the strength and stiffness of LWRT, and the best fiber length is approximately 80 mm in this situation.

Synergy between the Matrix and Fibers - Compatibilizer and Surface Matrix Layer

Independent fibers for stress transfer is not enough because there is no effective bonding between them. Thus, the matrix makes great contributions and improves the synergy between the matrix and fibers. The matrix in composites plays an important role in stress homogenization and stress transfer although fibers sustain most loads. Therefore, on a microscopic scale, good bonding between fibers and the matrix is required and on a macroscopic scale, the surface matrix

layer is also required to homogenize stress in LWRT.

The different polarities between glass fibers and polypropylene weaken the interfacial bonding without any modification. It is very helpful to add compatibilizers to the matrix to improve the strength and stiffness, and maleic anhydride grafted polypropylene (MAH-g-PP) [21] is the most commonly used compatibilizer. The non-woven process was employed to prepare LWRT with a surface density of 1400 g/m^2 and thickness of 4 mm. The matrix was blended with 7 % MAH-g-PP. Table 1 shows the comparison of mechanical properties between LWRT with and without MAH-g-PP. Both the tensile and flexural properties are greatly increased. The tensile strength increases by 50 % and the flexural modulus increases by 26.7 %. However, the notched impact strength drops by 67 %. This is because the matrix bonds the fibers together, and with the addition of MAH-g-PP, the bonding strength will increase and the fiber web will become stronger and stiffer. The resistance to deformation increases, such that it prefers to dissipate energy by direct fiber fracture than web strain and fiber pull-out. As shown in Figure 13, the bonding between the resin and fibers is closer and stronger. With the addition of MAH-g-PP, fiber fracture is observed explicitly with a neat section around these fibers. This indicates that LWRT tends to dissipate energy mainly by fiber fracture when the bonding is good. The top images in Figure 13 show the matrix without MAH-g-PP, and pull-out is easily observed and dissipates much more energy. It can be noted that the interfacial modification is a crucial factor of LWRT. The effects of compatibilizers on LWRT are more important than on traditional GMT because the matrix in GMT has more probability to be in contact with fibers, while the matrix in LWRT may be dilute in bonding fibers due to air interruption. Therefore, compatibilizers have the ability to improve the synergy between the matrix and fibers.

Table 1. Mechanical properties of LWRT with and without MAH-g-PP

Properties	Without MAH-g-PP	With 7 % MAH-g-PP
Tensile strength (MPa)	13.03±0.89	19.55±0.92
Tensile modulus (MPa)	1311±102	1614±121
Flexrual strength (MPa)	7.69±0.62	8.42±0.65
Flexrual modulus (MPa)	579.4±36.5	734.2±46.7
Notched izod impact strength (kJ/m^2)	26.59±1.32	8.77±0.72

It is not beneficial for exposed fibers to transfer and homogenize stress on surfaces of LWRT. Therefore, another measure to improve the synergy between the fibers and matrix is to add surface layers. The PP matrix can be used as the surface layer. Thus, the matrix distribution design in LWRT is also important to achieve good matrix surface layers. To investigate the effects of surface layer, the film stacking method was used. Different ratios between the surface film and interior film are adopted with the identical matrix content. The thickness ratios of the surface/interior/surface film were designed as 1:2:1 and 1:1:1. Using the same processing conditions, two types of LWRT obtained are distinguished as A and B, respectively. The surface matrix of B is richer than that of A, as shown in Figure 14. Table 2 lists the mechanical properties comparison between

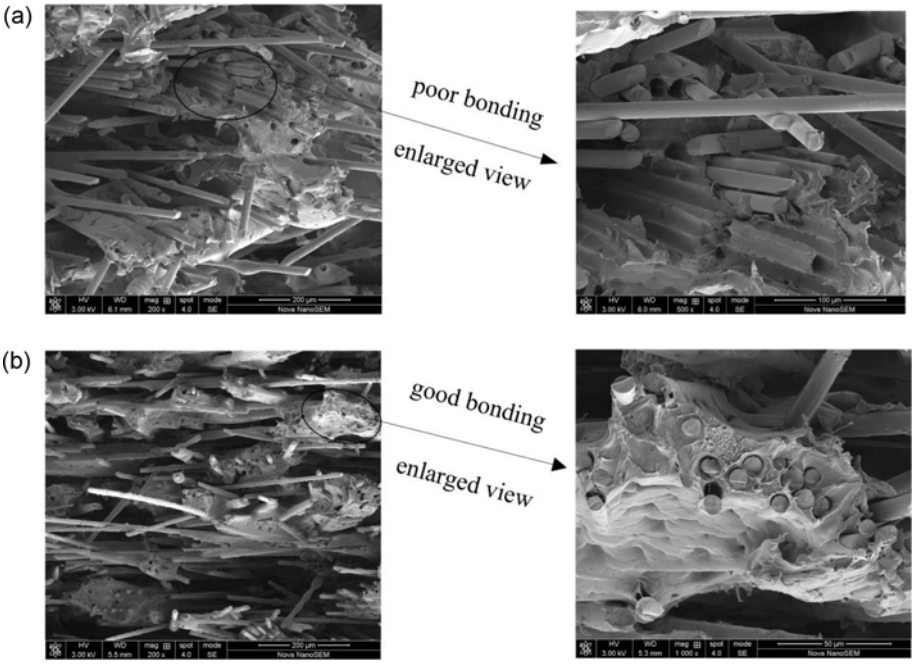

Figure 13. Impact fracture section (a) without MAH-g-PP and (b) with 7 % MAH-g-PP.

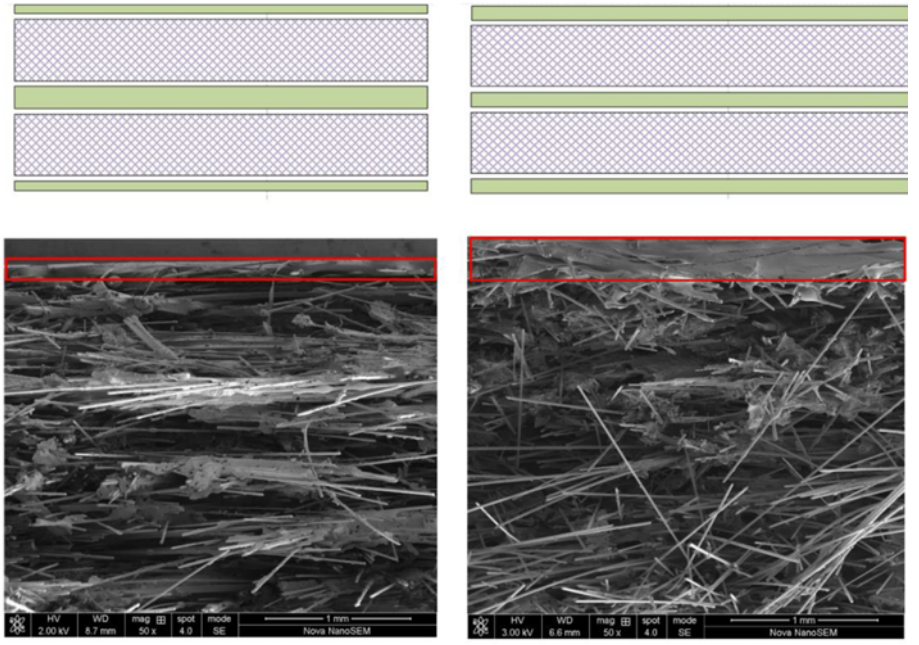

Figure 14. Comparison of surface matrix enrichment; (A) with less surface matrix and (B) with more surface matrix.

Table 2. Mechanical properties of A and B

Properties	A	B
Tensile strength (MPa)	21.92±1.25	23.06±1.42
Tensile modulus (MPa)	1851±102	2092±110
Flexrual strength (MPa)	9.68±0.87	11.26±1.01
Flexrual modulus (MPa)	568.4±34.5	603.8±44.5

A and B. It is found that the surface with more matrix exhibits higher strength and stiffness. The resin on the surface can distribute the stress from tensile or flexural load, such that the sustained force will transfer in the whole framework more uniformly to avoid the concentrated stress destruction. The results also imply that with surface layer enrichment, the stress transfer between fibers is more effective and the strength and stiffness of LWRT increase as well. It is also found that although materials with high strength and modulus are used as skins traditionally, PP matrix layers also have effects on reinforcing LWRT because compared with the porous material, PP may exhibit higher mechanical properties.

Conclusion

LWRT is a newly developed porous composite. Air is introduced as a structural element to reduce density and improve stiffness. The framework of LWRT is composed of fibers and matrix. Among all of the factors, the molded thickness and surface density have the greatest effects on the mechanical properties of LWRT. With higher thickness and lower surface density, the strength and modulus are decreased. This is because the porosity is increased and the introduced air interrupts the stress transfer within LWRT. However, the stiffness of LWRT exhibits a maximum value when its thickness reaches 4 mm. The increased stiffness is due to the increased inertia moment when the thickness of LWRT increases. The influence of fiber length is also important because stress transfer is interrupted in fiber reinforced cellular composites. It is found that a longer fiber length is required to transfer stress and increase strength in LWRT. The impact strength also increases with the fiber length under 80 mm. This is due to the deformation of fiber webs that can dissipate more energy. Synergy between fibers and matrix is important and may be enhanced by adding compatibilizers and the surface matrix layer. It is discovered that compatibilizers increase the tensile and flexural properties dramatically. The bonding strength of fibers and the matrix is enhanced by the effects of compatibilizers. However, the possibility of fiber breakage also increases, which is not beneficial to the impact strength of LWRT. Surface matrix enrichment also increases the strength and stiffness. The applied load is distributed and the stress is homogenized by the effects of the surface matrix layer.

Acknowledgements

We gratefully acknowledge the support of the National Natural Science Foundation of China (Grant No. 21376086).

References

1. E. Haque and S. Ickes, SAE 2000 World Congress, SAE International, Detroit, MI, United States, March 6-9, 2000.
2. J. Stange and H. Münstedt, *J. Cell. Plast.*, **42**, 445 (2006).
3. R. L. Heck, *J. Vinyl Add. Tech.*, **4**, 113 (1998).
4. C. Wang, S. Ying, and Z. Xiao, *J. Cell. Plast.*, **49**, 65 (2013).
5. A. K. Bledzki and O. Faruk, *J. Appl. Polym. Sci.*, **97**, 1090 (2005).
6. L. Vaikhanksi and S. R. Nutt, *Compos. Pt. A-Appl. Sci. Manuf.*, **34**, 755 (2003).
7. E. M. Wouterson, F. Y. Boey, X. Hu, and S.-C. Wong, *Compos. Sci. Technol.*, **65**, 1840 (2005).
8. L. Ye, M. Lu, and Y.-W. Mai, *Compos. Sci. Technol.*, **62**, 2121 (2002).
9. M. Lu, L. Ye, and Y.-W. Mai, *Compos. Sci. Technol.*, **64**, 191 (2004).
10. L. Ye, Z.-R. Chen, M. Lu, and M. Hou, *Compos. Pt. A-Appl. Sci. Manuf.*, **36**, 915 (2005).
11. J. Wolfrath, V. Michaud, and J.-A. Månson, *Compos. Sci. Technol.*, **65**, 1601 (2005).
12. J. Wolfrath, V. Michaud, and J.-A. Månson, *Compos. Pt. A-Appl. Sci. Manuf.*, **36**, 1608 (2005).
13. Y. Wan and J. Takahashi, *J. Reinf. Plast. Compos.*, **33**, 1613 (2014).
14. C. Harper and K. Kunal, 12th Annual Automotive Composites Conference and Exhibition, SPE Automotive and Composites Divisions, Troy, MI, United States, September 11-13, 2012.
15. H. Dittmar, 6th Annual SPE Automotive Composites Conference, Society of Petroleum Engineers, Troy, MI, United States, September 12-14, 2006.
16. S. Jespersen, M. Wakeman, V. Michaud, D. Cramer, and J.-A. Månson, *Compos. Sci. Technol.*, **68**, 1822 (2008).
17. B.-H. Lee, H.-S. Kim, S. Lee, H.-J. Kim, and J. R. Dorgan, *Compos. Sci. Technol.*, **69**, 2573 (2009).
18. J. Schell, M. Renggli, G. Van Lenthe, R. Müller, and P. Ermanni, *Compos. Sci. Technol.*, **66**, 2016 (2006).
19. B. Harris, "Engineering Composite Materials", pp.99-127, The Institute of Materials, London, 1999.
20. L. Vaikhanski, J. J. Lesko, and S. R. Nutt, *Compos. Sci. Technol.*, **63**, 1403 (2003).
21. J. Bian, X. W. Wei, H. L. Lin, I. T. Chang, and E. Sancaktar, *J. Appl. Polym. Sci.*, **130**, 3025 (2013).